

**A mechanistic model for anaerobic
phototrophs in domestic wastewater
applications: Photo-Anaerobic Model (PAnM)**

D. PUYOL^{a,b,c,}, E. BARRY^{a,b}, T. HUELSEN^{a,b}, D.J. BATSTONE^{a,b}.*

*9a Advanced Water Management Centre, Gehrmann Building, The
10University of Queensland, Brisbane, Queensland 4072, Australia*

*11b CRC for Water Sensitive Cities, PO Box 8000, Clayton, Victoria, 3800,
12Australia*

*13c Group of Chemical and Environmental Engineering (GIQA), University
14Rey Juan Carlos, 28933 Mostoles, Madrid, Spain*

15 Corresponding author information: daniel.puyol@urjc.es. Chemical and
16Environmental Engineering Group. University Rey Juan Carlos. Room 234.
17Departamental Building I (Mostoles), Mostoles Campus. C/ Tulipán, S/n,
1828933 - Mostoles - Madrid – Spain. Tel: +34 914888095 (ext. 8095), Fax:
19+34 914887086*

20

21JOURNAL SELECTED: WATER RESEARCH

22NUMBERING (without tables and figures): 7797 words

23NUMBER OF TABLES: 3

24NUMBER OF FIGURES: 6

25 **ABSTRACT**

26Purple phototrophic bacteria (PPB) have been recently proposed as a key
27potential mechanism for accumulative biotechnologies for wastewater treatment
28with total nutrient recovery, low greenhouse gas emissions, and a neutral to
29positive energy balance. Purple phototrophic bacteria have a complex
30metabolism which can be regulated for process control and optimization. Since
31microbial processes governing PPB metabolism differ from traditional processes

32used for wastewater treatment (e.g., aerobic and anaerobic functional groups in
33ASM and ADM1), a model basis has to be developed to be used as a framework
34for further detailed modelling under specific situations. This work presents a
35mixed population phototrophic model for domestic wastewater treatment in
36anaerobic conditions. The model includes photoheterotrophy, which is divided
37into acetate consumption and other organics consumption, chemoheterotrophy
38(including simplified fermentation and anaerobic oxidation) and photoautotrophy
39(using hydrogen as an electron donor), as microbial processes, as well as
40hydrolysis and biomass decay as biochemical processes, and is single-biomass
41based. The main processes have been evaluated through targeted batch
42experiments, and the key kinetic and stoichiometric parameters have been
43determined. The process was assessed by analysing a continuous reactor
44simulation scenario within a long-term wastewater treatment system in a photo-
45anaerobic membrane bioreactor.

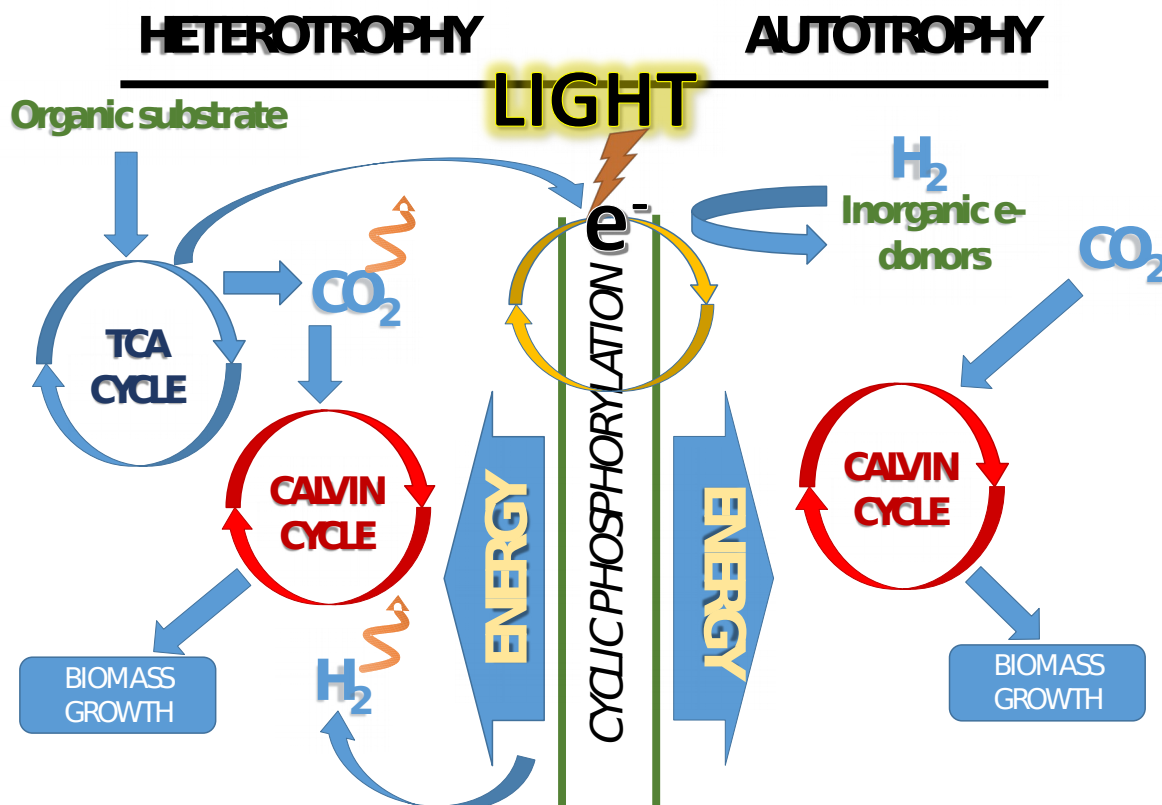
46Key words: *Phototrophic bacteria, resource recovery, mechanistic modelling,*
47*Partition-Release-Recovery*

48

49

50

51 Graphical Abstract



53 HIGHLIGHTS

- 55 - A mechanistic model for anaerobic phototrophs has been developed: PAnM
- 56 - The model includes organic C and H_2 (as COD) and inorganic C, N and P.
- 57 - Microbial processes based on PPB metabolism were identified through
- 58 dedicated experiments.
- 59 - Kinetic and stoichiometric parameters were determined in batch tests.
- 60 - Model was tested by simulating the process in a photo-anaerobic MBR

611 INTRODUCTION

62 Wastewater treatment is shifting focus to include the capture and recovery of
 63 organics and nutrients. This requires novel technological approaches. A key
 64 approach is the use of fast growing organisms to concentrate energy, nutrients,
 65 and trace compounds into the solid phase, and hence substantially reduce
 66 reactive removal of nitrogen and organics while enabling phosphorous recovery.
 67 One option is high-rate activated sludge, which can achieve 40% nitrogen
 68 removal in the primary stage through adsorption and assimilation (Jetten et al.
 69 1997). Algae can also be used to partition to the solid phase, but a simultaneous

70heterotrophic and photosynthetic mode is generally enabled by bacterial-algal
71associations that reduce organic substrate consumption efficiency (Muñoz and
72Guieysse 2006). Purple phototrophic bacteria (PPB) present a new partitioning
73approach, which has been shown to completely remove nitrogen to discharge
74limits when sufficient organic carbon is present without the need for pure
75cultures, and using infra-red (IR)light only as a driver for growth (Hulsen et al.
762014).

77PPB grow phototrophically rather than photosynthetically, and do not use water
78as an electron donor to produce oxygen and organics. They are among the most
79metabolically versatile organisms on earth (Hunter et al. 2008). They grow
80heterotrophically using a wide range of organic compounds, both in presence
81and absence of light (photoheterotrophy and chemoheterotrophy) (Hunter et al.
822008). However, they can also grow autotrophically by using infrared light as the
83energy driver for CO₂ fixation, and with inorganic electron donors such as H₂,
84Fe²⁺, S²⁻ or S₂O₃²⁻ (cyclic anoxygenic photosynthesis) (Overmann and Garcia-
85Pichel 1998). Although they can grow in the presence of oxygen, they are
86extremely effective in anaerobic photoheterotrophic conditions (Gordon and
87McKinlay 2014, McKinlay and Harwood 2010). Their ability to recycle electrons
88during the cyclic anoxygenic photosynthesis gives them the ability to harvest
89and retain electrons, as well as a high energetic efficiency. They can even
90accumulate electrons in the form of reduced cofactors which enable the disposal
91of electrons. This can be done through two main strategies: (i) ATP-driven
92hydrogen production by ferredoxin oxidation in the hydrogenase/nitrogenase
93system at the end of the electron transport chain (ETC), and (ii) the increase of
94assimilative growth by re-fixation of CO₂ via the Calvin Cycle produced during
95heterotrophic metabolism (McKinlay and Harwood 2010). These metabolic
96features give them the possibility of growing and out-competing other
97heterotrophic microorganisms where light is present, including in low to medium
98strength wastewater systems with short hydraulic retention times (HRT) (Hulsen
99et al. 2014).

100PPB have a number of additional metabolic functions useful in wastewater
101treatment systems. They are able to accumulate polymers such as poly-
102phosphate (poly-P) (Liang et al. 2010), polysaccharides (Klein et al. 1991), poly-β
103hydroxybutyrate (PHB) (Melnicki et al. 2009) and other poly-
104(hydroxyalkanoates) (PHA) (Brandl et al. 1991). Under an excess of organics

105and available energy, and in the absence of mineral nitrogen, they generate
106hydrogen and fix nitrogen as ammonia (Basak and Das 2007).

107PPB have been assessed for wastewater treatment, particularly for processing
108swine (Kim et al. 2004), latex rubber-sheet (Kantachote et al. 2005), tofu (Zhu
109et al. 1999), and sugar refinery wastewaters (Yetis et al. 2000). However, most of
110these studies were focused on hydrogen production rather than organics
111removal or nutrient recovery (Fang et al. 2005, Lee et al. 2010, Tao et al. 2008).
112They have also been applied to domestic wastewater (DWW) in batch and
113continuous operation to completely remove nitrogen to discharge limits (Hulsen
114et al. 2014). This process enables a single-step treatment of wastewater with
115HRT and effluent qualities similar to those of activated sludge processes without
116destroying nitrogen and phosphorus.

117Modelling is used to design, benchmark, and analyse wastewater treatment
118systems, with the IWA Activate Sludge Model (ASM) family models being the
119most widely used for conventional activated sludge processes (Henze et al.
1202006). The IWA anaerobic digestion model no. 1 (ADM-1) is the analogous model
121for domestic and industrial anaerobic systems (Batstone et al. 2002). The IWA
122Models, and wastewater modelling in general has generally applied first order
123hydrolysis for solids transformation (including decay), Monod for uptake kinetics
124and inverse Monod (non-competitive) for inhibition functions, with a COD basis
125for organics and molar basis for inorganic compounds. Development of new
126technologies such as PPB requires development of a similar mechanistic model.

127There are complex metabolic models based on PPB metabolism primarily focused
128on the electron transport chain (Golomysova et al. 2010, Klamt et al. 2002). Due
129to their complexity, these models are motivated more by a need for a
130mechanistic understanding of the underlying process rather than field
131applications. These models are therefore unsuitable for a wastewater model. In
132particular, they include components which can't be measured readily, making
133validation difficult. They also lack capability outside the core application area.
134There has also been work done on modelling PPB to describe hydrogen
135production (Eroglu 2008, Gadhamshetty et al. 2008, Obeid et al. 2009),. In
136contrast, due to the domestic wastewater matrix, the key growth modes are
137photoheterotrophy (principal) as well as chemoheterotrophy and
138photoautotrophy. Biochemical processes relevant to complex substrates such
139as solids hydrolysis and biomass decay must be considered as well. Therefore,

this work aims to propose a mechanistic model for mixed culture PPB as a partition agent in DWW treatment with adaptability to treatment of industrial wastewaters.

2 Materials and Methods

2.1 Model Description

The model was developed to be unit-compatible with the IWA ASM and ADM series (Batstone et al. 2002, Henze et al. 2006). Therefore, units of mgCOD L^{-1} (or gCOD m^{-3}) for both soluble and particulate organics were chosen. Nutrient units are in mgN L^{-1} and mgP L^{-1} , respectively, with inorganic carbon (IC, HCO_3^-) in molC L^{-1} .

Monod kinetics is uniformly applied for biological growth processes, with first order kinetics for hydrolysis and decay. Monod or non-competitive inhibition has been applied for limiting or inhibitory expressions respectively. Due to a lack of functional differentiation within the PPB clade, and limited evidence to the contrary, only one biomass component has been selected (PPB). Other biological groups present in ASM and ADM1 models (e.g., hydrogen utilising methanogens, denitrifiers or fermentative bacteria) could be readily included. As in the ASM/ADM models S_i is used for soluble compounds, and X_i for particulate compounds, where subscript i denotes the compound.

The model does not currently include poly-P or other polymer accumulation, since this occurs mainly in static growth mode (Hiraishi et al. 1991, Liang et al. 2010) complexity. Likewise, nitrification/denitrification processes are not included, since they can only occur in aerobic conditions where ammonia can be oxidized to nitrite or nitrate. Therefore, N and P are removed by assimilative growth only.

In the presence of organic substrates and IR light, photoheterotrophy through the tri-carboxylic acid (TCA) cycle is assumed to dominate. Two major mechanisms of electron disposal by PPB are considered. Firstly, the production of CO_2 (S_{IC}) is a key feature of PPB biomass under growth conditions (McKinlay and Harwood 2010) and is important for closing the C balance. The oxidation state of the organic compound determines if the biomass fixes CO_2 for substrate uptake and electron balance (in the case of reduced substrates such as propionate, butyrate or valerate), or the uptake produces CO_2 (in the case of oxidized

173 substrates such as acetate, succinate or ethanol) (McKinlay and Harwood 2011).
 174 In the latter case, the biomass disposes of excess of electrons by re-fixing the
 175 CO_2 produced in the TCA cycle. As a consequence, there is usually limited
 176 consumption or production of CO_2 in domestic wastewater. A theoretical
 177 explanation of this mechanism is explained in Supplementary Information (SI).
 178 The other major mechanism of electron disposal by PPB is H_2 production via the
 179 nitrogenase complex. In static growth mode, the PPB biomass is able to use the
 180 excess of electrons for redox balance at the end of the ETC. The ferredoxin
 181 complex is the carrier for this process, but the biomass needs energy in the form
 182 of ATP (Golomysova et al. 2010). However, this process is inhibited in presence
 183 of NH_4^+ , a strong inhibitor of the nitrogenase activity (Rodionov et al. 1986).
 184 Indeed, H_2 production is inhibited in a DWW fed situation due to (i) presence of
 185 ammonium and (ii) disposing of electrons by CO_2 re-fixation which promotes
 186 growth (see SI for more details). Therefore, it can be deduced that CO_2
 187 production and re-fixation into the Calvin Cycle is the major electron sink in PPB
 188 metabolism. In the absence of organic substrates, autotrophic growth is the sole
 189 growth mode, using reduced inorganic compounds other than water as electron
 190 donor (anoxygenic photosynthesis). In the interest of model simplification and
 191 considering domestic wastewater contains generally low sulfur levels, the sulfur
 192 cycle has been omitted. It is however possible to add sulfate reduction into the
 193 model with subsequent sulfide utilisation as an electron donor for autotrophic
 194 PPB growth. This would require the addition of another biomass component (PPB
 195 cannot perform sulfate reduction). PPB can perform chemoheterotrophy at a
 196 lower rate, providing H_2 (S_{h2}) for photoautotrophy (Golomysova et al. 2010).

197 Transforming these mechanisms to a model enables the following key processes
 198 (Figure 1):

- 199 (i) *Photoheterotrophy on acetate (S_{ac}) (acetate uptake)*: This involves
 200 acetate assimilation by PPB in the presence of infra-red radiation
 201 Acetate is treated separately from the other substrates due to
 202 differences observed during batch tests. Due to an imbalance in
 203 substrate-biomass carbon oxidation state, this process also results in
 204 production of CO_2 .
- 205 (ii) *Photoheterotrophy on other organics (S_s) (photoheterotrophic uptake)*:
 206 These include all soluble organics that PPB can assimilate for growth in
 207 the presence of infra-red radiation. Compounds include VFAs excluding

acetate, alcohols, and some sugars. These have been lumped into a single soluble substrate. Similar to (i) this results in the uptake of CO₂.

(iii) *Chemoheterotrophy (chemoheterotrophic uptake)*: This process involves the assimilative consumption of any organic in dark conditions that can be metabolized through either fermentation or anaerobic oxidation processes. All these processes have been joined as one process for a shake of simplicity. This process involves H₂ and acetate as end products. Acetate is not further oxidised through chemoheterotrophy due to a lack or very limited terminal electron acceptors such as Fe(III) and sulfate (Finneran et al. 2003).

(iv) *Photoautotrophy (autotrophic uptake)*: This process involves assimilative CO₂ fixation by PPB in the presence of infra-red radiation using H₂ as the electron donor. Other electron donors such as Fe²⁺, S²⁻ and S₂O₃⁻ have been omitted but could be included.

(v) *PPB cell death (decay)*: This process involves the deactivation of PPB by cell death. Ammonium, phosphate and inorganic carbon are released and the biomass is converted into biodegradable organic particulates (X_s) and particulate inerts (X_i).

(vi) *Hydrolysis and particulate fermentation (hydrolysis)*: The decomposition of biodegradable particulates into organics (S_{ac} and S_s), ammonium, phosphate, hydrogen and inorganic carbon is addressed as a sole process for simplicity. Both soluble and particulate inerts are also products of this process. A breakdown of particulate fermentation could be incorporated into the model e.g. for processes with long solids retention times (SRT).

The model is presented in Petersen matrix notation in Table 1. Kinetic parameters were generally obtained from the batch experiments, or from the literature in specific cases as described below. The saturation constant for hydrogen consumption by photoautotrophic process (K_{S,h2}) light limitation (K_{S,E}) and inhibition by ammonia (K_{i,FA}) were set arbitrarily low since affinity is high (Chen et al. 2008, Uyar et al. 2007). Stoichiometry was determined by both theoretical calculations from literature, and experimentally. The model is balanced over COD, C, N and P. HCO₃⁻, NH₄⁺ and PO₄²⁻ have been used for closing C, N and P balances, respectively.

Extra information regarding all aspects of model development and implementation can be found in the supplementary information (SI) and codes can be found on the UQ repository (LINK). SI1 includes the description of model components, full kinetic parameters and stoichiometric coefficients. The determination and calibration of stoichiometry is included in SI2, and SI4 contains the full list of model equations.

2.2 Batch Experiments

Batch experiments were done to identify parameters based on the developed model. Detailed experimental methods are provided in the SI. The inoculum was sourced from a lab-scale continuous photo-anaerobic membrane bioreactor (PAnMBR) described by (Hülßen et al. 2016b) operated over 300 d. Domestic wastewater was collected from the Taringa wastewater lift station (Brisbane, Australia) with an average strength of 572 mgCOD L⁻¹ and soluble COD of 241 mgCOD L⁻¹, 63 mgN L⁻¹, and 9 mgP L⁻¹.

Where wastewater was not the medium, synthetic Ormerod medium was used at pH 7.5 as described previously (Hülßen et al. 2014).

Metabolic growth batch tests: All batch tests were done in 100 mL working volumes (160 mL serum flasks) in triplicate, inoculated from the PAnMBR reactor. The headspace was flushed with N₂ and experiments were carried out at 20°C in an orbital shatter at 150 rpm (Edwards Instrument Company). The array of flasks was irradiated with 150W lamps using UV-VIS absorbing foil as described elsewhere (Hülßen et al. 2014). All experiments were accompanied blank samples with no substrate, and by positive and negative controls where necessary. A summary is provided in Table 2.

Hydrolysis and biomass decay: The inoculum (0.5 L) was collected as per the above method (2.1 g VSS L⁻¹). The biomass was centrifuged in 50 mL Falcon tubes and the pellet resuspended again in NaCl 0.2 M three times. Biomass was then placed in 0.5 L of NaCl 0.2 M and was divided into two 0.25 L Schott bottles, which were subsequently flushed with N₂ and magnetically stirred at 200 rpm. The bottles were operated for 30 d.

One of the bottles was covered with aluminium foil to avoid phototrophic activity, and was used for the hydrolysis analysis. Liquid sampling was performed twice a week to analyse volatile fatty acids (VFAs), NH₄-N, PO₄-P, total inorganic carbon

275(TIC) and pH. Headspace was analysed for CH₄, H₂ and CO₂. TSS/VSS, TKN and TP
276was analysed every 7 d.

277The other bottle was illuminated as indicated above without feed, and biomass
278samples were taken every 7 d to assess activity (determining decay coefficient).
279Activity tests were done as above with 100 mgCOD L⁻¹ of acetate and 10 mg NH₄-
280N L⁻¹.

281*Calculation of Specific Phototrophic Activities (SPA).* Non-linear parameter
282estimation is generally used to determine parameters as described in 2.4.2, but
283specific phototrophic activity was also determined by linear regression of
284substrate concentration over a minimum of four points through the region of
285maximum consumption divided by biomass concentration.

2862.3 Analytical methods

287Total COD (TCOD) and soluble COD (SCOD) were determined by COD cell tests
288(Merck, 1.14541.0001, Darmstadt, Germany). Dissolved NH₄⁻-N, NO₂-N and PO₄-P
289were determined by a QuikChem8000 Flow Injection Analyzer (FIA) (Hach
290Company, Loveland, USA). Temperature and pH were measured using an Oakton
291pH 11 Series (Vernon Hill, IL, USA). TSS and VSS were determined by filtration
292according to standard methods, where TSS were calculated after drying the
293sample in an oven at 105 ± 2 °C and VSS were calculated after burning it in a
294furnace at 550 ± 5 °C (APHA. 1998). Illuminance (W m⁻²) was measured with an
295IR light sensor (PAS Port™, Roseville, CA, USA). VFA samples were analysed by
296gas chromatography (Agilent Technologies 7890A GC System, Santa Clara, CA,
297USA) equipped with a flame ionisation detector (GC/FID) and a polar capillary
298column (DB-FFAP). Gas samples were analysed by GC (2014 Shimadzu, Kyoto,
299Japan) with thermal coupled detector (TCD) (Tait et al. 2009). TKN and TP were
300determined using sulfuric acid, potassium sulfate and copper sulfate catalyst in a
301block digester (Lachat BD-46, Hach Company, Loveland, CO, USA) (Patton and
302Truitt 1992). TIC was analysed by using a total organic carbon (TOC) analyser
303(Shimadzu TOC-L CSH TOC Analyser with TNM-L TN unit) coupled to a near
304infrared detector (NIRD) for measuring the CO₂. All soluble constituents were
305determined after filtering with a 0.45 µm membrane filter (Millipore, Millex®-HP,
306Merck Group, Darmstadt, Germany).

3072.4 Data analysis

3082.4.1 Data handling

309Biomass concentration was calculated in g VSS L⁻¹, and it was further
310transformed into COD by using the COD relationship calculated from the biomass
311equation CH_{1.8}O_{0.38}N_{0.18} (McKinlay and Harwood 2010) (1 g biomass expressed as
312VSS = 1.78 g COD).

313Biomass yields (Y) were calculated accounting for the initial and final biomass
314concentration (in g VSS L⁻¹) based on substrate consumption. Biomass
315concentration was further transformed into COD and then yields are expressed
316as mgCOD_{biomass} mgCOD⁻¹.

3172.4.2 Statistical analyses

318All parameters were estimated from triplicate batch/measurements by
319minimisation of residual sum of squares (J=RSS). Parameter uncertainty was
320determined using two-tailed *t*-tests calculated from standard error in parameter
321value, obtained from the Fisher information matrix. Where parameter
322optimisation problems involve multiple parameters (k_M , K_S), parameter
323uncertainty surface ($J=J_{crit}$) has also been assessed as described in (Batstone et
324al. 2003) . Confidence intervals (at 95%) were also calculated based on two-
325tailed *t*-tests from parameter standard error, as above, and used for statistical
326representative comparisons. Error bars in experimental data represent 95%
327confidence intervals in mean based on a two-tailed *t*-test (5% significance
328threshold). Uncertainty of the slope for the analysis of SPA was analysed in Excel
329using Data Analysis. Standard error in slope was subsequently converted into
33095% confidence interval. All statistical analyses were done with a 5% significance
331threshold.

3322.5 Simulation of a continuous PAnMBR

333The resulting kinetic expressions were used in the development of a continuous
334PAnMBR model. As previously demonstrated, the concentration of the
335bioavailable SCOD in medium strength domestic wastewater is insufficient for
336the system to achieve total nitrogen and total phosphorous discharge limits
337(Hülßen et al. 2016b). To achieve full removal, additional SCOD is required.

338The goals of the simulation were the following: a) to highlight the requirement of
339additional SCOD to achieve total nutrient removal, and b) to demonstrate that
340the inclusion of a primary clarifier before can lead to a product enriched in PPB.

341Dynamic influent data was simulated according to the influent generator model
342developed by Gernaey et al. (2011), and adapted to the typical concentrations
343of primary influent reported by Hülsen et al., 2014. Based on the average
344influent characteristics and an HRT of 12 h, volumetric loading rate (VLR) of 1400 ± 12 mg COD L⁻¹ d⁻¹ and a solid retention time (SRT) of 3 d, a reactor volume of
34670 m³ was applied. An ideal primary clarifier was included, with a solids removal
347efficiency of 60%±3% Tchobanoglous et al. (2003).

348Simulation and subsequent data processing were done in Matlab (MATLAB
349R2015a, The MathWorks Inc., Natick, MA). As the system of equations is stiff, the
350system of ordinary differential equations was solved by ODE15s. The case was
351simulated for 600 days with 3 stages of differing SCOD concentrations. The
352dynamic influent after settling was applied directly during Stage I until day 300.
353During Stage II (days 300-450), acetate was added to the optimum COD/N/P ratio
354of 100/7.1/1.8 based on the limiting nutrient (N or P). During Stage III, acetate
355addition was ceased. This was to assess process response to a sudden change,
356and to demonstrate that the system requires wastewater with a specific COD/N/
357P ratio. . State equations were implemented in a fixed volume, completely mixed
358membrane bioreactor.

359The results from the simulation were balanced over COD, N, P and C, and have
360been included in the SI.

361The Matlab function and run files, along with their supporting datasets, have
362been uploaded to <http://espace.library.uq.edu.au/view/UQ:412280>.

3633 Results

364The sludge used for all the experiments came from a lab-scale PAnMBR (Hülsen
365et al. 2016b). Most of the microorganisms are related with *α-proteobacteria*, PPB
366accounting for more than 70% of the total gene copies detected by the
367pyrosequencing technique. The genus *Rhodobacter* ssp. is the most abundant,
368representing more than 60% of the microbiota (Hülsen et al. 2016b). The
369presence of photosynthetic organisms such as microalgae and cyanobacteria
370accounts for less than 1% of total gene copies. Therefore, the biomass can be
371considered as PPB-dominant biomass.

3723.1 Growth Processes

373Photoheterotrophy was assessed with VFAs and ethanol as substrate (Fig 2a). All
374substrates were completely consumed during the experiment, and overall yields
375were similar in all cases, with an average biomass yield of $1.13 \pm 0.21 \text{ mg}$
376 $\text{COD}_{\text{biomass}} \text{ mg}^{-1} \text{ COD}$. More details are provided in the SI. As can be seen in Figure
3772b, uptake rates of substrates excluding acetate were similar, with a k_M of $1.3 \pm$
378 $0.1 \text{ (mgCOD mgCOD}^{-1} \text{ d}^{-1})$, and undetectable K_S . Acetate had a significantly higher
379 k_M ($2.4 \pm 0.2 \text{ mgCOD mgCOD}^{-1} \text{ d}^{-1}$) and detectable, albeit low, K_S of $20 \pm 4 \text{ mgCOD}$
380 L^{-1} . This essentially means that growth (uptake) is faster on acetate, but with a
381lower affinity such that acetate uptake is faster at the beginning of the batch,
382but slower at the end.

383The analysis of chemoheterotrophic metabolism by PPB was conducted by using
384acetate and ethanol as substrates in dark conditions (Figure 2c). PPB biomass
385was much less effective in dark conditions compared with light conditions
386(biomass yield 0.5 vs $1.1 \text{ mg COD}_{\text{biomass}} \text{ mg}^{-1} \text{ COD}$ in dark and light conditions,
387respectively). Biomass yield in dark conditions is relatively high compared to
388typical values reported in literature for dark fermentation and anaerobic
389oxidation processes, which are rarely greater than $0.2 \text{ mg COD}_{\text{biomass}} \text{ mg}^{-1} \text{ COD}$
390(Batstone et al. 2002). The occurrence of energy storage (particularly poly-P)
391may have a significant role here due to batch operation (Liang et al. 2010). The
392maximum uptake rate, is approximately half that of photoheterotrophy (Figure
3932d), though with again, extremely low K_S values. While chemotrophic growth is
394not dominant under photoheterotrophic conditions, it can be very important to
395consider in reactor design (e.g., where there is insufficient light), and also for
396balancing COD, C, N and P.

397Analysis of photoautotrophy was done with NaHCO_3 as C source and Na_2S as
398electron donor in 5-fold stoichiometric excess (see Table 2) (Figure 2e). The
399biomass had a yield of $36,000 \text{ mg COD}_{\text{biomass}} \text{ mol}^{-1} \text{ C}$ comparable to the value on
400acetate ($31,560 \text{ mgCOD}_{\text{biomass}} \text{ mol}^{-1} \text{ C}$). However, maximum uptake rate was far
401lower at $3.4 \pm 0.2 \times 10^{-6} \text{ molC mgCOD d}^{-1}$ (compared to $75 \pm 2 \times 10^{-6} \text{ molC mgCOD}$
402 d^{-1} on acetate) (Figure 2f). Photoautotrophy needs to be considered for when
403there is an excess of bicarbonate and electrons from inorganic sources in the
404wastewater. It is also important to consider photoautotrophy in order to close
405mass balances. This case is particularly relevant in light deficiency, where

406fermentation and anaerobic oxidation processes may become important and
407hence H_2 is available as a major electron source for PPB.

408Nutrient limitation experiments for N and P were used to determine saturation
409coefficients for N and P. K_s values were extremely low such that the N and P
410regulation became a switch function (data shown in SI). Biomass assimilated
411nutrients at a COD/N/P ratio of 100/7.1/1.8, which is higher than conventional
412aerobic bacteria and much higher than other anaerobes (Tchobanoglous et al.
4132003). These values are in line with previous works (Hulsen et al. 2014).
414However, PPB were able to grow at a lower rate once the nutrients were
415completely consumed (42% lower than in full nutrient conditions), likely due to
416fixation of headspace N_2 (Hunter et al. 2008) (inhibited in the presence of
417ammonium). Also, PPB can accumulate polymers such as poly-P (Liang et al.
4182010) as well as PHA (Melnicki et al. 2009), which can be used in static growth
419mode. Since the model developed here is sustained on biomass growth in
420presence of nitrogenase inhibiting ammonium, nutrient limitation for growth
421must be included.

4223.2 Endogenous processes – hydrolysis and decay

423Hydrolysis and decay are considered as transversal first order biochemical
424processes in most models (Batstone et al. 2006, Henze et al. 2006, Szilveszter et
425al. 2010). These could be considered separately, since phototrophic growth can
426be restricted in the absence of irradiance, and decay can be determined directly
427by measurement of phototrophic activity following periods of irradiation without
428substrate. Figure 3 shows the time series of the SPA values (on acetate)
429calculated for the PPB biomass during starvation. Biomass activity reduced
430according to a first order model with decay coefficient of $0.09 \pm 0.02 \text{ d}^{-1}$.
431Hydrolysis was assessed in dark conditions with substrate present, to avoid
432reassimilation of products by PPB. Therefore, hydrolysis products (organic C
433sources as COD, inorganic C as HCO_3^- , N as NH_4^+ and P as PO_4^{3-}) could be
434measured and were directly correlated with first order kinetics of the hydrolytic
435process. Hydrolysis also followed a first order model with a hydrolysis coefficient
436of $0.071 \pm 0.002 \text{ d}^{-1}$ (Fig 4). It should be noted that hydrolysis is substrate
437specific, and is highly situation specific (Batstone et al. 2015), but that a value of
438close to 0.1 d^{-1} is comparable with hydrolysis kinetics under anaerobic conditions,
439but much lower than that for aerobic processes (Henze et al., 2006).

4404 Discussion

4414.1 Parameter values vs pure culture PPB

442A full list of parameter values can be found in the SI, whereas Table 3 shows
443parameters determined from the literature in comparison with those reported
444here. Parameters were calculated on the basis that (i) protein composition of PPB
445is in all cases 60% of dry weight (McKinlay and Harwood 2010), (ii) 1 g VSS =
4461.78 g COD and (iii) PPB biomass equation is $\text{CH}_{1.8}\text{O}_{0.38}\text{N}_{0.18}$ (McKinlay and
447Harwood 2010).

448In general, biomass yields calculated here are in line with values reported in the
449literature (Table 3). The only exception is the biomass yield for autotrophic
450growth, where no relevant values have been found and only indirect calculation
451can be performed. Wang et al. (1993) reported biomass growth and CO_2 fixation
452in *Rhodobacter sphaeroides* and *Rhodospirillum rubrum* using different electron
453sources (H_2 , thiosulfate, sulphide and malate) and the biomass yield values
454extracted from their activities vary considerably with an average value of 84,000
455mg COD mol^{-1} C fixed. These values, however, did not consider re-fixation of CO_2
456from malate that may underestimate considerably real CO_2 usage for growth in
457the Calvin cycle (McKinlay and Harwood 2011). Therefore the biomass yield
458differs from the value reported here ($36,100 \pm 850$ mg COD mol^{-1} C fixed). The
459value determined during this study is however very close to the theoretical
460maximum yield for carbon dioxide fixation of 39,840 mg COD mol^{-1} C, and as
461such, is a reasonable value.

462However, specific uptake rates were substantially different to the literature
463values depending on the growth mechanism, which may be due to use of pure
464cultures in contrast with mixed cultures used in the present work. Generally,
465chemoheterotrophic parameters, pure cultures have an activity close to two
466orders of magnitude higher than the mixed culture in this work. This results in
467activities similar to those of typical fermentative bacteria. An example is found
468in (Schultz and Weaver 1982) where the growth rates of *Rhodospirillum rubrum*
469and *Rhodopseudomonas capsulata* were studied on several chemoheterotrophic
470substrates in the dark. The authors used trimethylamine-N-oxide as accessory
471electron acceptor on fructose, glucose and succinate, likely removing electron
472management as a major limitation. Photoheterotrophic parameters also
473diverged depending on the substrate. While acetate uptake rates were similar to
474the values reported here (Golomysova et al. 2010, McKinlay and Harwood 2011),

475those obtained from other organics, such as malate (Gadhamshetty et al. 2008,
476Klein et al. 1991), lactate + malate (Obeid et al. 2009), or butyrate (McKinlay and
477Harwood 2011) were almost one order of magnitude higher. These parameters
478were obtained in hydrogen production studies. Under these situations, the
479substrate uptake is optimized for biogenic H₂ by dislocating catabolism from
480anabolism due to excess of electrons. This increases considerably the substrate
481uptake rate while minimising yield (Basak and Das 2007). In this work, the μ_{max}
482for photoheterotrophic metabolism was calculated to be 1.54 d⁻¹, which
483corresponds to a doubling time of 0.45 d. It is similar to those reported by
484McKinlay and Harwood (2011) (0.27-0.44 d), and generally aligns well with purple
485phototrophic bacteria (Hunter et al. 2008). The use of pure cultures promotes
486specific uptake rates to the detriment of substrate affinity. This leads to
487increased k_M and K_S parameters, a typical behaviour of r-strategist
488microorganisms (Dorodnikov et al. 2009).

489Hydrolysis and decay rates dependent the particulate substrate hydrolysing, and
490the system redox conditions. In general, for a given material, the hydrolysis
491coefficient increases from anaerobic to anoxic, and from anoxic to aerobic
492(Henze et al. 2006). The biomass decay and hydrolysis constants found in
493literature were obtained in aerobic photoheterotrophic processes (Huang et al.
4941999, Huang et al. 2001),.This explains considerably higher values than those
495calculated here.

496Compared with previous analyses, this study is focused on mixed culture
497photoheterotrophic metabolism. The biomass seems to be a K-strategist which
498promotes substrate affinity over uptake, a microbial strategy in low-strength
499systems as domestic wastewater with low hydraulic retention times (less than 12
500h). Such behaviour is useful for out-competing other fast-growing
501microorganisms. It is clearly effective when compared to the slow growing
502methanogens, which are the only competitors for acetate under anaerobic
503conditions with low concentrations of sulfate or reduced metals (Dorodnikov et
504al. 2009). Indeed, PPB microorganisms have been demonstrated to prevail and
505dominate in continuous PAnMBR reactors treating real domestic wastewater
506without previous inoculation, both in mesophilic (Hülsen et al. 2016b) as well as
507in psychrophilic (Hülsen et al. 2016a) conditions.

5084.2 Model application

509The model was tested in a realistic scenario, with influent profile generated using
510the BSM influent generator (Gernaey et al. 2011). Detailed information about the
511simulations is provided in the SI.

5124.2.1 Fate of C, N and P

513The model indicates different SCOD removal efficiencies for particular periods of
514operation. In general, adaptation to seasonal periods of variable wastewater
515composition is rapid, as can be shown in input values from Figures 5 and 6. For
516periods (I) and (III), which correspond to no additional acetate in the system
517(average inlet SCOD of $290.2 \pm 0.5 \text{ mg COD L}^{-1}$), the mean SCOD removal
518efficiency is 87% (Figure 5a) The remaining SCOD in the system can be almost
519entirely attributed to the presence of non-biodegradable SCOD, accounting for
52097% of the effluent SCOD. During period (II) acetate was added to agree with the
521COD/N/P requirements for PPB. Average SCOD removal efficiency remained
522almost invariable at around 87% due to optimized COD/N/P conditions. As in the
523Stage I, almost all the remaining SCOD corresponded to soluble inerts. The
524model, however, is not able to reproduce the PPB behaviour under a high excess
525of inlet SCOD concentration since it is based on assimilative mechanisms only
526and accumulation processes are not included, as e.g. PHA or glycogen. The PPB
527biomass is able to accumulate these compounds (Brandl et al. 1991, Melnicki et
528al. 2009), and so SCOD removal efficiencies are expected to be higher and less
529dependent on nutrients in real cases (Hülsen et al. 2016a, Hülsen et al. 2016b).
530An upgraded model including accumulative mechanisms is therefore needed for
531high COD:N ratio wastewater. However, this model is suitable for normal DWW
532treatment operation, where N and P are generally in excess.

533Nutrient assimilation was directly linked with biomass growth. The optimum
534assimilative COD/N/P relationship has been calculated to be 100/7.1/1.8 from
535batch experiments. Therefore, periods with non-optimal ratios are expected to
536have higher effluent nutrient concentrations. Under normal situation (periods (I)
537and (III)), with no additional acetate, nutrients were not completely removed and
538ammonium and phosphate efficiencies were 47% and 59%, respectively (Figures
5395b and 5c, respectively). This justifies the need for extra SCOD addition, as has
540been previously described experimentally (Hülsen et al. 2016b). Phosphorus was
541almost completely removed during C and N sufficiency during period (II), with
542removal efficiencies of 93%. However, depletion of P prevented a high N

removal due to nutrient imbalance, and so N removal efficiencies during these period averaged 74%. Again, accumulative mechanisms may have a key role here, as PPB are able to accumulate poly-P (Liang et al. 2010). This mechanism is quite complex and has not been properly defined, particularly in mixed cultures and on wastewater sources.

Production of biomass was related to PPB growth as well as input solids. Biomass fractionation (X_{PB} , X_S and X_I) along the simulation period is depicted in Figure 6. When acetate was not added, PPB biomass was produced at 44% of the total biomass in the outlet (sludge line). Adding acetate increased this value up to 53% of total biomass. Accumulation of X_S within the reactor is a direct consequence of slow hydrolysis due to low HRT. Additional substrate increased biomass concentration due to assimilation of remnants of N and P. This also boosted the SRT and decay was more evident, increasing X_S concentrations up to values above 1000 mgCOD L⁻¹ (see stage (II) in Figure 6). Inerts fraction, however, was always below 23% of the total particulates concentration, probably due to the slow hydrolysis rate. Increasing substrate addition not only caused a net increase of PPB concentration inside the reactor due to assimilative growth on the remnant N and P, but also caused an increase of SRT and decay was gaining importance. This was traduced in increasing X_S concentrations until achieving values above 1000 mg COD L⁻¹ (see stage (II) in Figure 6). However, inerts fractionation was always below 23% of the total biomass exiting the reactor, which is explained by the slow hydrolysis rate. These results have an important effect on energy distribution in the PRR platform since all energy balances are directly related with the biomass management through anaerobic digestion, and the relative amount of PPB will influence potential anaerobic degradability and biomass consistency. An important aspect identified by this continuous analysis is that the biomass fraction X_{PB} is always relatively small, even when applying a settler (compared with activated sludge streams predicted by the ASM1). This is because the hydrolysis coefficient is very low (<0.1 d⁻¹) compared with the levels of >2 d⁻¹ typically applied in the ASM1-2d (Henze et al. 2006). This means that while growth rates are comparable to activated sludge, hydrolysis rates are far lower, and hence metabolic activity is dominated by available soluble substrate (and possibly N and P) rather than electron acceptor availability. In any case, there will always be a large proportion of undegraded particulates, due to the slow hydrolysis coefficient, and in a stable, solids dominated system, PPB sludge

578should be more analogous to primary sludge rather than activated sludge, with
579both negative and positive consequences.

580Simulation of biomass behaviour has implications on biomass production upon
581main line biological treatment. There is a net increment of biomass production
582yield compared to typical activated sludge processes. This could have an impact
583in energy recovery (through biogas) but also in sludge waste disposal expenses,
584which can be partially counteracted by downstream production of high value-
585added bioresources as proteins, prebiotics and probiotics (Matassa et al. 2015)
586or bioplastics (Padovani et al. 2016), as well as energetic resources as third
587generation liquid biofuels (Castro et al. 2016).

588

5895 Conclusions

590Anaerobic phototrophic growth in domestic wastewater treatment is fast,
591comparable to activated sludge (in k_M values) with very low K_S values, indicating
592that purple phototrophic bacteria behave as K strategist. However, hydrolysis is
593relatively slow ($\sim 0.1 \text{ d}^{-1}$), which means that particulate substrates will not be
594degraded at short HRTs. The predominant mechanism is photoheterotrophy, with
595autotrophy and chemotrophy generally slow. The decay rate is relatively high,
596comparable to activated sludge under aerobic conditions. The dynamics under
597continuous conditions indicate that biological processes are adaptable to normal
598flow variations such that performance at a given mode is stable.

599The model has the following limitations:

- 600 (i) The model is only valid for anaerobic conditions, and hydrogen
601 production for redox balancing is assumed to be inhibited, so this
602 model cannot be implemented for hydrogen production systems as it
603 is.
- 604 (ii) poly-P and other polymers accumulation is not included due to a lack of
605 foundational research. Also, nitrogen fixation is not included since it is
606 assumed to be inhibited by ammonium.
- 607 (iii) Detailed pH simulation is needed, particularly for batch processes,
608 where pH is likely to vary due to removal of acids.

609A key priority should be inclusion of poly-P and PHA accumulation as well as N_2
610fixation and side H_2 production, as these processes (poly-P without carbon, PHA

without oxidation of organics, and N_2/H_2 production) are unique to photoanaerobic organisms.

6 ACKNOWLEDGEMENTS

This work was jointly funded by the Smart Water Fund (project 100S-023) and the CRC for Water Sensitive Cities (project C2.1). Thanks are given to Prof. James B. McKinlay for his kind discussion on PPB metabolism.

7 REFERENCES

APHA., 1998. Standard Methods for the Examination of Water and Wastewater. 20th ed. American Public Health Association, Washington, DC, USA.

Basak, N. and Das, D., 2007. The prospect of purple non-sulfur (PNS) photosynthetic bacteria for hydrogen production: the present state of the art. World Journal of Microbiology and Biotechnology 23(1), 31-42.

Batstone, D.J., Keller, J., Angelidaki, I., Kalyuzhnyi, S., Pavlostathis, S., Rozzi, A., Sanders, W., Siegrist, H. and Vavilin, V., 2002. The IWA Anaerobic Digestion Model No 1(ADM 1). Water Science & Technology 45(10), 65-73.

Batstone, D.J., Keller, J. and Steyer, J., 2006. A review of ADM 1 extensions, applications, and analysis: 2002-2005. Water Science and Technology 54(4), 1-10.

Batstone, D.J., Pind, P.F. and Angelidaki, I., 2003. Kinetics of thermophilic, anaerobic oxidation of straight and branched chain butyrate and valerate. Biotechnol Bioeng 84(2), 195-204.

Batstone, D.J., Puyol, D., Flores-Alsina, X. and Rodríguez, J., 2015. Mathematical modelling of anaerobic digestion processes: applications and future needs. Reviews in Environmental Science and Bio/Technology 14(4), 595-613.

Brandl, H., Gross, R.A., Lenz, R.W., Lloyd, R. and Fuller, R.C., 1991. The accumulation of poly(3-hydroxyalkanoates) in Rhodobacter sphaeroides. Archives of Microbiology 155(4), 337-340.

Castro, A.R., Rocha, I., Alves, M.M. and Pereira, M.A., 2016. Rhodococcus opacus B4: a promising bacterium for production of biofuels and biobased chemicals. AMB Express 6(1).

Chen, Y., Cheng, J.J. and Creamer, K.S., 2008. Inhibition of anaerobic digestion process: A review. Bioresource Technology 99(10), 4044-4064.

Dorodnikov, M., Blagodatskaya, E., Blagodatsky, S., Fangmeier, A. and Kuzyakov, Y., 2009. Stimulation of r- vs. K-selected microorganisms by elevated atmospheric CO₂ depends on soil aggregate size: Research article. FEMS Microbiology Ecology 69(1), 43-52.

647Eroglu, I., 2008. Hydrogen production by *Rhodobacter sphaeroides* O.U.001 in a
648flat plate solar bioreactor. *International Journal of Hydrogen Energy* 33(2), 531-
649541.

650Fang, H.H.P., Liu, H. and Zhang, T., 2005. Phototrophic hydrogen production from
651acetate and butyrate in wastewater. *International Journal of Hydrogen Energy*
65230(7), 785-793.

653Finneran, K.T., Johnsen, C.V. and Lovley, D.R., 2003. *Rhodoferrax ferrireducens*
654sp. nov., a psychrotolerant, facultatively anaerobic bacterium that oxidizes
655acetate with the reduction of Fe(III). *International Journal of Systematic and*
656*Evolutionary Microbiology* 53(3), 669-673.

657Gadhamshetty, V., Sukumaran, A., Nirmalakhandan, N. and Theinmyint, M.,
6582008. Photofermentation of malate for biohydrogen production— A modeling
659approach. *International Journal of Hydrogen Energy* 33(9), 2138-2146.

660Gernaey, K.V., Flores-Alsina, X., Rosen, C., Benedetti, L. and Jeppsson, U., 2011.
661Dynamic influent pollutant disturbance scenario generation using a
662phenomenological modelling approach. *Environmental Modelling & Software*
66326(11), 1255-1267.

664Golomysova, A., Gomelsky, M. and Ivanov, P.S., 2010. Flux balance analysis of
665photoheterotrophic growth of purple nonsulfur bacteria relevant to biohydrogen
666production. *International Journal of Hydrogen Energy* 35(23), 12751-12760.

667Gordon, G.C. and McKinlay, J.B., 2014. Calvin cycle mutants of
668photoheterotrophic purple nonsulfur bacteria fail to grow due to an electron
669imbalance rather than toxic metabolite accumulation. *J Bacteriol* 196(6), 1231-
6701237.

671Henze, M., Gujer, W., Mino, T. and Van Loosedrecht, M., 2006. Activated sludge
672models ASM1, ASM2, ASM2d and ASM3.

673Hiraishi, A., Yanase, A. and Kitamura, H., 1991. Polyphosphate Accumulation by
674*Rhodobacter sphaeroides* Grown under Different Environmental
675Conditions with Special Emphasis on the Effect of External Phosphate
676Concentrations. *Bulletin of Japanese Society of Microbial Ecology* 6(1), 25-32.

677Huang, J.S., Jih, C.G. and Sung, T.J., 1999. Performance enhancement of
678suspended-growth reactors with phototrophs. *Journal of Environmental*
679*Engineering* 125(6), 501-507.

680Huang, J.S., Wu, C.S., Jih, C.G. and Chen, C.T., 2001. Effect of addition of
681*Rhodobacter* sp. to activated-sludge reactors treating piggery wastewater. *Water*
682*Res* 35(16), 3867-3875.

683Hülßen, T., Barry, E.M., Lu, Y., Puyol, D. and Batstone, D.J., 2016a. Low
684temperature treatment of domestic wastewater by purple phototrophic bacteria:
685Performance, activity, and community. *Water Research* 100, 537-545.

686Hülßen, T., Barry, E.M., Lu, Y., Puyol, D., Keller, J. and Batstone, D.J., 2016b.
687Domestic wastewater treatment with purple phototrophic bacteria using a novel
688continuous photo anaerobic membrane bioreactor. *Water Research* 100, 486-
689495.

690Hulsen, T., Batstone, D.J. and Keller, J., 2014. Phototrophic bacteria for nutrient
691recovery from domestic wastewater. *Water research* 50, 18-26.

692Hunter, C.N., Daldal, F., Thurnauer, M.C. and Beatty, J.T., 2008. *The Purple*
693*Phototrophic Bacteria*, Springer.

694Jetten, M.S.M., Horn, S.J. and van Loosdrecht, M.C.M., 1997. Towards a more
695sustainable municipal wastewater treatment system. *Water Science and*
696*Technology* 35(9), 171-180.

697Kantachote, D., Torpee, S. and Umsakul, K., 2005. The potential use of
698anoxygenic phototrophic bacteria for treating latex rubber sheet wastewater.
699*Electronic Journal of Biotechnology* 8(3), 314-323.

700Kim, M.K., Choi, K.-M., Yin, C.-R., Lee, K.-Y., Im, W.-T., Lim, J.H. and Lee, S.-T.,
7012004. Odorous swine wastewater treatment by purple non-sulfur bacteria,
702*Rhodopseudomonas palustris*, isolated from eutrophicated ponds. *Biotechnology*
703*letters* 26(10), 819-822.

704Klamt, S., Schuster, S. and Gilles, E.D., 2002. Calculability analysis in
705underdetermined metabolic networks illustrated by a model of the central
706metabolism in purple nonsulfur bacteria. *Biotechnol Bioeng* 77(7), 734-751.

707Klein, G., Klipp, W., Jahn, A., Steinborn, B. and Oelze, J., 1991. The relationship of
708biomass, polysaccharide and H₂ formation in the wild-type and *nifA/nifB* mutants
709of *Rhodobacter capsulatus*. *Archives of Microbiology* 155(5), 477-482.

710Lee, H.-S., Vermaas, W.F. and Rittmann, B.E., 2010. Biological hydrogen
711production: prospects and challenges. *Trends Biotechnol* 28(5), 262-271.

712Liang, C.-M., Hung, C.-H., Hsu, S.-C. and Yeh, I.-C., 2010. Purple nonsulfur
713bacteria diversity in activated sludge and its potential phosphorus-accumulating
714ability under different cultivation conditions. *Applied Microbiology and*
715*Biotechnology* 86(2), 709-719.

716Madigan, M.T. and Gest, H., 1978. Growth of a photosynthetic bacterium
717anaerobically in darkness, supported by "oxidant-dependent" sugar
718fermentation. *Archives of Microbiology* 117(2), 119-122.

719Matassa, S., Batstone, D.J., Hülsen, T., Schnoor, J. and Verstraete, W., 2015. Can
720direct conversion of used nitrogen to new feed and protein help feed the world?
721*Environmental Science and Technology* 49(9), 5247-5254.

722McKinlay, J.B. and Harwood, C.S., 2010. Carbon dioxide fixation as a central
723redox cofactor recycling mechanism in bacteria. *Proceedings of the National*
724*Academy of Sciences of the United States of America* 107(26), 11669-11675.

725McKinlay, J.B. and Harwood, C.S., 2011. Calvin cycle flux, pathway constraints,
726and substrate oxidation state together determine the H₂ biofuel yield in
727photoheterotrophic bacteria. *MBio* 2(2), e00323-00310.

728Melnicki, M.R., Eroglu, E. and Melis, A., 2009. Changes in hydrogen production
729and polymer accumulation upon sulfur-deprivation in purple photosynthetic
730bacteria. *International Journal of Hydrogen Energy* 34(15), 6157-6170.

731 Muñoz, R. and Guieysse, B., 2006. Algal–bacterial processes for the treatment of
732 hazardous contaminants: A review. *Water Research* 40(15), 2799-2815.

733 Obeid, J., Magnin, J., Flaus, J., Adrot, O., Willison, J. and Zlatev, R., 2009.
734 Modelling of hydrogen production in batch cultures of the photosynthetic
735 bacterium *Rhodobacter capsulatus*. *International Journal of Hydrogen Energy*
736 34(1), 180-185.

737 Overmann, J. and Garcia-Pichel, F., 1998. The phototrophic way of life: The
738 Prokaryotes: an evolving electronic resource for the microbiological community.
739 M. Dworkin, New York, Springer.

740 Padovani, G., Carlozzi, P., Seggiani, M., Cinelli, P., Vitolo, S. and Lazzeri, A., 2016.
741 PHB-rich biomass and BioH₂ production by means of photosynthetic
742 microorganisms, pp. 55-60.

743 Patton, C.J. and Truitt, E.P., 1992. Methods of Analysis by the US Geological
744 Survey National Water Quality Laboratory: Determination of the Total
745 Phosphorus by a Kjeldahl Digestion Method and an Automated Colorimetric Finish
746 that Includes Dialysis, US Geological Survey.

747 Rodionov, Y.V., Lebedeva, N.V. and Kondratieva, E.N., 1986. Ammonia inhibition
748 of nitrogenase activity in purple and green bacteria. *Archives of Microbiology*
749 143(4), 345-347.

750 Sarles, L.S. and Tabita, F.R., 1983. Derepression of the synthesis of D-ribulose 1,
751 5-bisphosphate carboxylase/oxygenase from *Rhodospirillum rubrum*. *J Bacteriol*
752 153(1), 458-464.

753 Schultz, J. and Weaver, P., 1982. Fermentation and anaerobic respiration by
754 *Rhodospirillum rubrum* and *Rhodopseudomonas capsulata*. *J Bacteriol* 149(1),
755 181-190.

756 Seitz, H.J., Schink, B., Pfennig, N. and Conrad, R., 1990. Energetics of syntrophic
757 ethanol oxidation in defined chemostat cocultures - 1. Energy requirement for H₂
758 production and H₂ oxidation. *Archives of Microbiology* 155(1), 82-88.

759 Szilveszter, S., Ráduly, B., Ábrahám, B., Lányi, S. and Niculae, D.R., 2010.
760 Mathematical models for domestic biological wastewater treatment process.
761 *Environmental Engineering and Management Journal* 9(5), 629-636.

762 Tait, S., Tamis, J., Edgerton, B. and Batstone, D.J., 2009. Anaerobic digestion of
763 spent bedding from deep litter piggery housing. *Bioresource technology* 100(7),
764 2210-2218.

765 Tao, Y., He, Y., Wu, Y., Liu, F., Li, X., Zong, W. and Zhou, Z., 2008. Characteristics
766 of a new photosynthetic bacterial strain for hydrogen production and its
767 application in wastewater treatment. *International Journal of Hydrogen Energy*
768 33(3), 963-973.

769 Tchobanoglous, G., Burton, F.L., Stensel, H.D., Metcalf and Eddy, 2003.
770 *Wastewater Engineering: Treatment and Reuse*, McGraw-Hill Education.

771Uyar, B., Eroglu, I., Yücel, M., Gündüz, U. and Türker, L., 2007. Effect of light
772intensity, wavelength and illumination protocol on hydrogen production in
773photobioreactors. International Journal of Hydrogen Energy 32(18), 4670-4677.

774Wang, X., Modak, H.V. and Tabita, F.R., 1993. Photolithoautotrophic growth and
775control of CO₂ fixation in Rhodobacter sphaeroides and Rhodospirillum rubrum in
776the absence of ribulose biphosphate carboxylase-oxygenase. J Bacteriol
777175(21), 7109-7114.

778Yetis, M., Gündüz, U., Eroglu, I., Yücel, M. and Türker, L., 2000. Photoproduction
779of hydrogen from sugar refinery wastewater by Rhodobacter sphaeroides OU
780001. International Journal of Hydrogen Energy 25(11), 1035-1041.

781Zhu, H., Suzuki, T., Tsygankov, A.A., Asada, Y. and Miyake, J., 1999. Hydrogen
782production from tofu wastewater by Rhodobacter sphaeroides immobilized in
783agar gels. International Journal of Hydrogen Energy 24(4), 305-310.

784

785TABLES

786**Table 1.** Petersen matrix of the PAM-1 model for domestic wastewater
787treatment by PPB.

Component (C) →		<i>i</i>	1	2	3	4	5	6	7	8	9	10
<i>j</i>	Process ↓		S_S	S_{ac}	S_{IC}	S_{h2}	S_{IN}	S_{IP}	S_I	X_{PB}	X_S	X_I
1	Hydrolysis/ fermentation		$f_{ss, xs}$	$f_{Sac, xs}$	$f_{IC, xs}$	$f_{h2, xs}$	$f_{IN, xs}$	$f_{IP, xs}$	$f_{Si, xs}$	0	-1	$f_{xi, xs}$
2	Acetate uptake		0	-1	$f_{IC, ph, ac}$	0	$f_{N, B} Y_{PB, ph}$	$f_{P, B} Y_{PB, ph}$	0	$Y_{PB, ph}$	0	0
3	Photoheterotroph ic uptake		-1	0	$-f_{IC, ph, Ss}$	0	$f_{N, B} Y_{PB, ph}$	$f_{P, B} Y_{PB, ph}$	0	$Y_{PB, ph}$	0	0
4	Chemoheterotro phic uptake		-1	$(1 - Y_{PB, ch}) f_{ac, ch}$	0	$(1 - Y_{PB, ch}) f_{h2, ch}$	$f_{N, B} Y_{PB, ch}$	$f_{P, B} Y_{PB, ch}$	0	$Y_{PB, ch}$	0	0
5	Autotrophic uptake		0	0	$-f_{IC, a}$	$f_{h2, a}$	$f_{N, B} Y_{PB, a}$	$-f_{P, B} Y_{PB, a}$	0	$Y_{PB, a}$	0	0
6	Decay of XPB		0	0	$-\sum_{i=8-9} C_i$	0	$-\sum_{i=8-9} C_i$	$-\sum_{i=8-9} C_i$	0	-1	1	0

Soluble substrate (mg COD L ⁻¹)
Acetate (mg COD L ⁻¹)
Inorganic carbon (mg COD L ⁻¹)
H ₂ (mg COD L ⁻¹)
Inorganic nitrogen (mg N_NH ₄ L ⁻¹)
Inorganic phosphorus (mg P_PO ₄ L ⁻¹)
Soluble inert (mg COD L ⁻¹)
Phototrophic biomass (mg COD L ⁻¹)
Biodegradable particulate (mg COD L ⁻¹)
Particulate inert (mg COD L ⁻¹)

Table 2: Batch conditions of the different metabolic tests.

Mechanism	Medium	Buffer system*	COD/N/P (C/N/P)***	C source (mgCOD L ⁻¹)	Electron donor (mg L ⁻¹)	Electron acceptor	Positive control	Negative control
Photoheterotrophy	Ormerod	HEPES	100/10/2	Acetate (130), propionate, butyrate, ethanol (100)	Organic	CO ₂	Adding 1 g NaHCO ₃	-
Nitrogen limitation	Ormerod	HEPES	100/1.4/2	Acetate (130)	Organic	CO ₂	No N limitation	-
Phosphorus limitation	Ormerod	HEPES	100/10/0.15	Acetate (130)	Organic	CO ₂	No P limitation	-
Photoautotrophy	Ormerod	Phosphate	(100/20/∞)	NaHCO ₃ (0.012)**	Na ₂ S (300)	CO ₂	-	No Na ₂ S
Chemoheterotrophy (dark)	Ormerod	HEPES	100/10/2	Ethanol (60), Acetate (130)	Organic	Acetate	With light	-
Inhibition of H ₂ production	DWW	-	100/12/4	DWW (278)	Organic	CO ₂	-	Acetate (600)
	Ormerod	Phosphate	100/15/∞	Acetate (600)	Organic	CO ₂	-	N limitation (1/10)

790* Buffer systems: HEPES (5.9 g L⁻¹), Phosphate (0.9 g K₂HPO₄ + 0.66 g KH₂PO₄). ** mol C L⁻¹ *** ∞ means in high
791excess due to buffering

792

Table 3: Comparison of estimated parameters with those reported in the literature.

Parameter	Units	Estimated values				Literature values			Ref s.	
$k_{M,ac}$	mg COD mg ⁻¹ COD d ⁻¹	2.4				1.5 (0.5), n=2			1	
$k_{M,ph}$	mg COD mg ⁻¹ COD d ⁻¹	1.4				11 (13), n=12			2	
$k_{M,ch}$	mg COD mg ⁻¹ COD d ⁻¹	0.074				5 (4), n=8			3	
$k_{M,ic}$	mol IC g ⁻¹ COD d ⁻¹	3.4 10 ⁻⁶				2.5 10 ⁻⁵ (1.7 10 ⁻⁵), n= 9			4	
$K_{S,s}$	mg COD L ⁻¹	0.5				4,333 (6,036), n=2			5	
$Y_{PB,ph}$	mg COD mg ⁻¹ COD	1.1				0.78 (0.37), n=17			6	
$Y_{PB,ch}$	mg COD mg ⁻¹ COD	0.5				0.23 (0.12), n= 8			7	
$Y_{PB,a}$	mg COD mg ⁻¹ C	36,100				132,000 (84,000), n=4			8	
k_{hyd}	d ⁻¹	0.07				0.27 (0.06), n=2			9	
k_{dec}	d ⁻¹	0.09				0.2 (0.02), n=2			10	
	$k_{M,ac}$ mg- COD mg ⁻¹ - COD d ⁻¹	$k_{M,ph}$ mg- COD mg ⁻¹ - COD d ⁻¹	$k_{M,ch}$	$k_{M,ic}$ mol- IC-g ⁻¹ - COD- d ⁻¹	$K_{S,s}$ mg- COD- L ⁻¹	$Y_{PB,ph}$ mg- COD- mg ⁻¹ - COD	$Y_{PB,ch}$ mg- COD mg ⁻¹ COD	$Y_{PB,a}$ mg- COD- mg ⁻¹ -C	k_{hyd} d ⁻¹	k_{dec} d ⁻¹
Estimated	2.4	1.4	0.074	3.4 10 ⁻⁶	0.5	1.1	0.5	36100	0.0 7	0.0 9
Literature average	1.5	11	5	2.5 10 ⁻⁵	4333	0.78	0.23	13200 0	0.2 7	0.2 0
Standard- deviation	0.5	13	4	1.7 10 ⁻⁵	6036	0.37	0.12	84000	0.0 6	0.0 2
n- (observation s)	2	12	8	9		17	8	4	2	
References	1	2	3	4	5	6	7	8	9	10

795¹ (Golomysova et al. 2010, McKinlay and Harwood 2011), ² (Gadhamshetty et al.
7962008, Golomysova et al. 2010, Klein et al. 1991, McKinlay and Harwood 2011,
797Obeid et al. 2009), ³ (Madigan and Gest 1978, Schultz and Weaver 1982), ⁴
798(Sarles and Tabita 1983, Wang et al. 1993), ⁵ (Gadhamshetty et al. 2008, Obeid
799et al. 2009), ⁶ (Gadhamshetty et al. 2008, Klamt et al. 2002, Klein et al. 1991,
800McKinlay and Harwood 2011, Obeid et al. 2009, Schultz and Weaver 1982), ⁷
801(Madigan and Gest 1978, Schultz and Weaver 1982), ⁸ (Wang et al. 1993), ⁹
802(Huang et al. 1999, Huang et al. 2001), ¹⁰ (Huang et al. 1999, Huang et al. 2001)

804 **FIGURE CAPTIONS**

805

806 **Figure 1:** Schematic summary of PPB metabolism under domestic wastewater
807 treatment. Key: N₂ase: Nitrogenase complex. TCA-c: Tri-carboxylic acid cycle.
808 DF: Dark fermentation. VFA: volatile fatty acids. e⁻: electrons. Dash: electron
809 cycles. Dot: proton pumps. *: Model components.

810 **Figure 2:** Experimental (symbols) and modelled (lines) time course of substrates
811 uptake (left) and parameters determination including 95% confidence intervals
812 and confidence regions (right) of PPB metabolism in photoheterotrophy (a),
813 chemoheterotrophy (b) and photoautotrophy (c) growth modes.

814 **Figure 3:** Mechanism of decay rate. Time course of specific phototrophic activity
815 of PPB subjected to starvation under full illumination.

816 **Figure 4:** Time course of released products upon starvation in dark conditions
817 demonstrating hydrolysis: soluble organic compounds but acetate (squares),
818 acetate (diamonds), hydrogen (triangles), TIC (pluses), NH₄⁺-N (circles) and PO₄³⁻-
819 P (crosses).

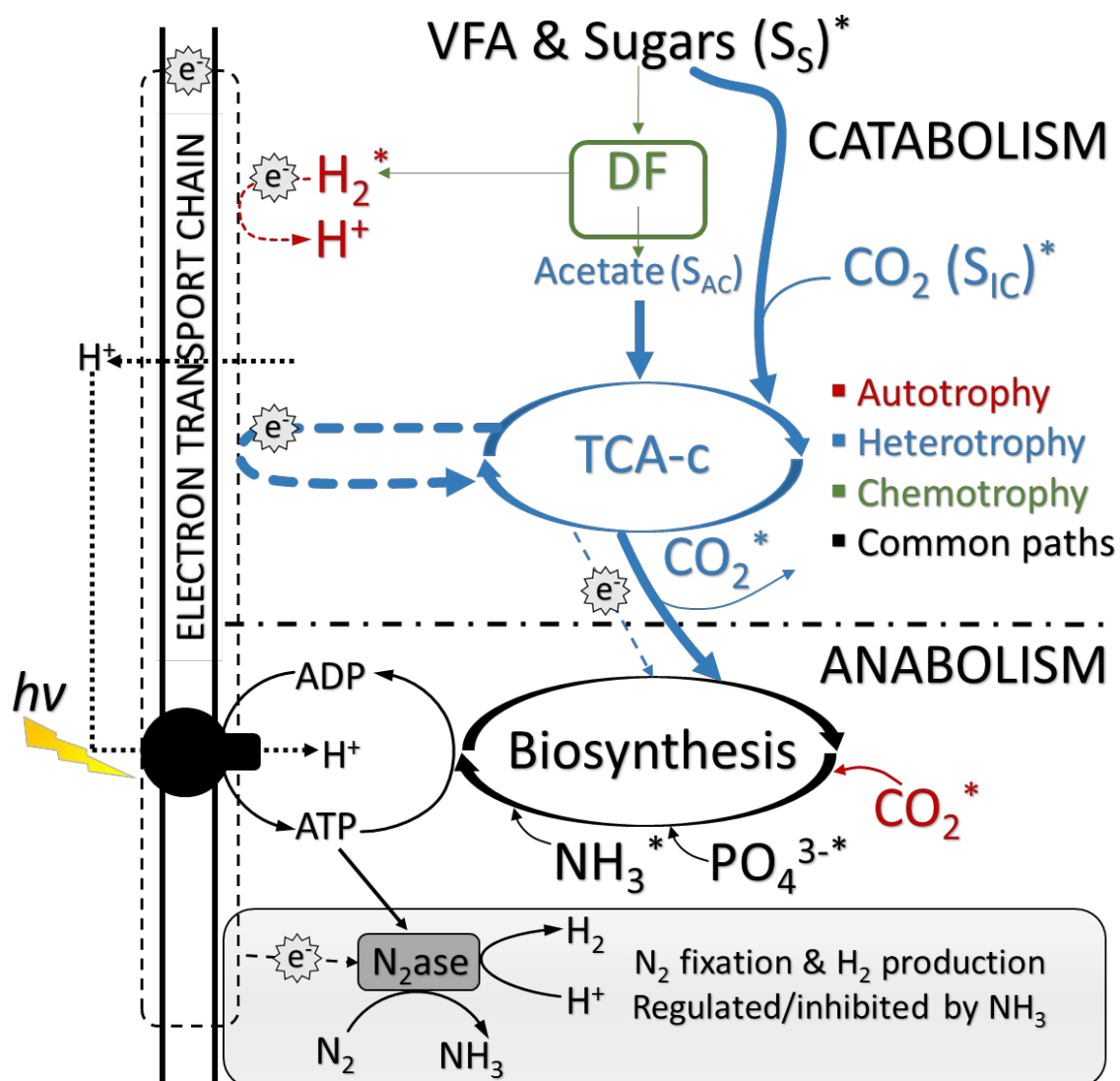
820 **Figure 5:** Influent (continuous line) and effluent concentrations (dash line) over
821 time for PAnMBR simulation for SCOD (a), ammonium (b) and phosphate (c) upon
822 primary settling. Different operational periods are indicated as vertical shades
823 separators.

824 **Figure 6:** Biomass fractionation including active phototrophic bacteria (dash
825 line), biodegradable particulate biomass (continuous line) and inert particulate
826 (dot lines) over time for the PAnMBR continuous simulation. Different operational
827 periods are indicated as vertical shades separators.

828

829

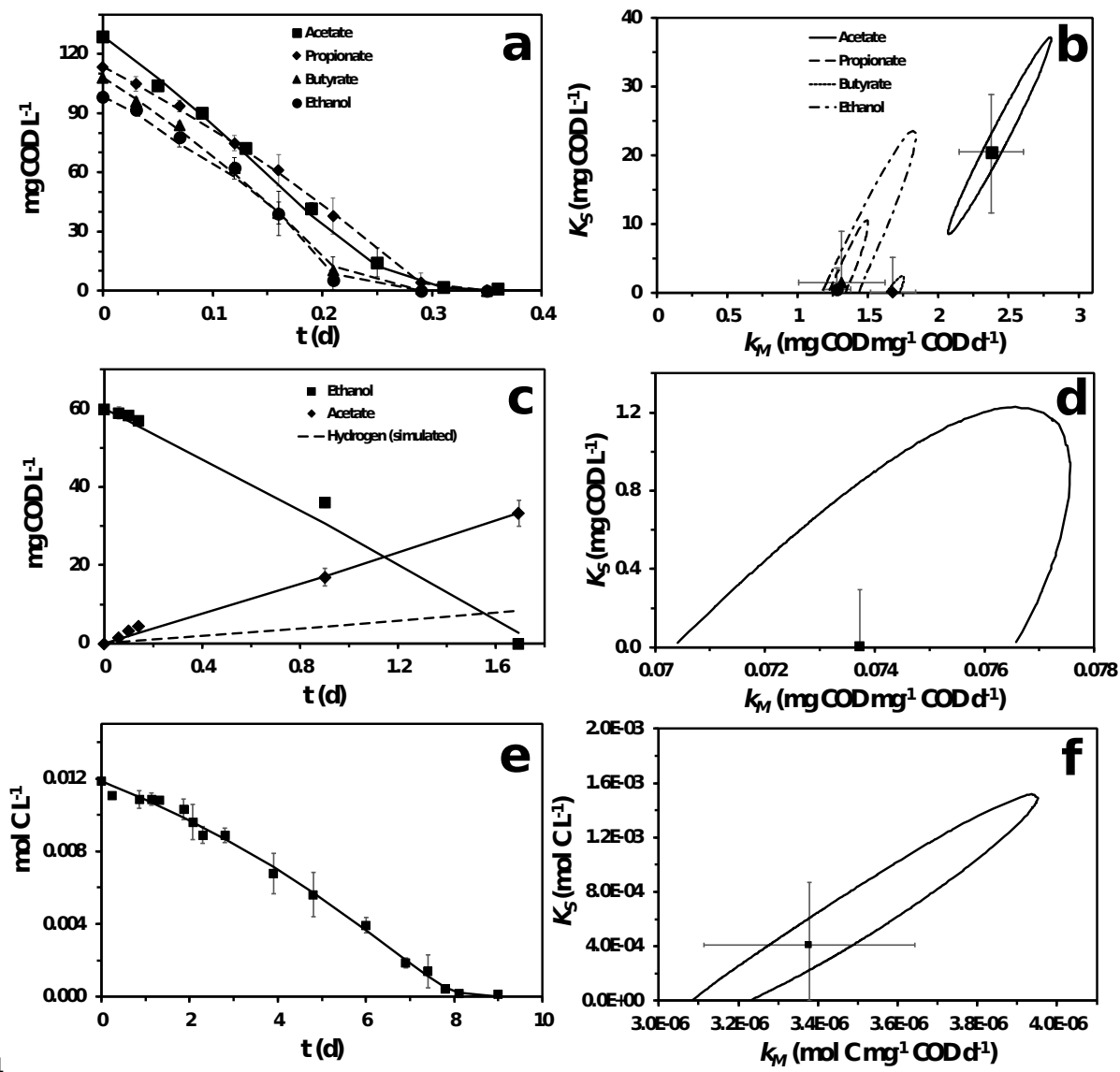
830 **FIGURE 1**



831

832

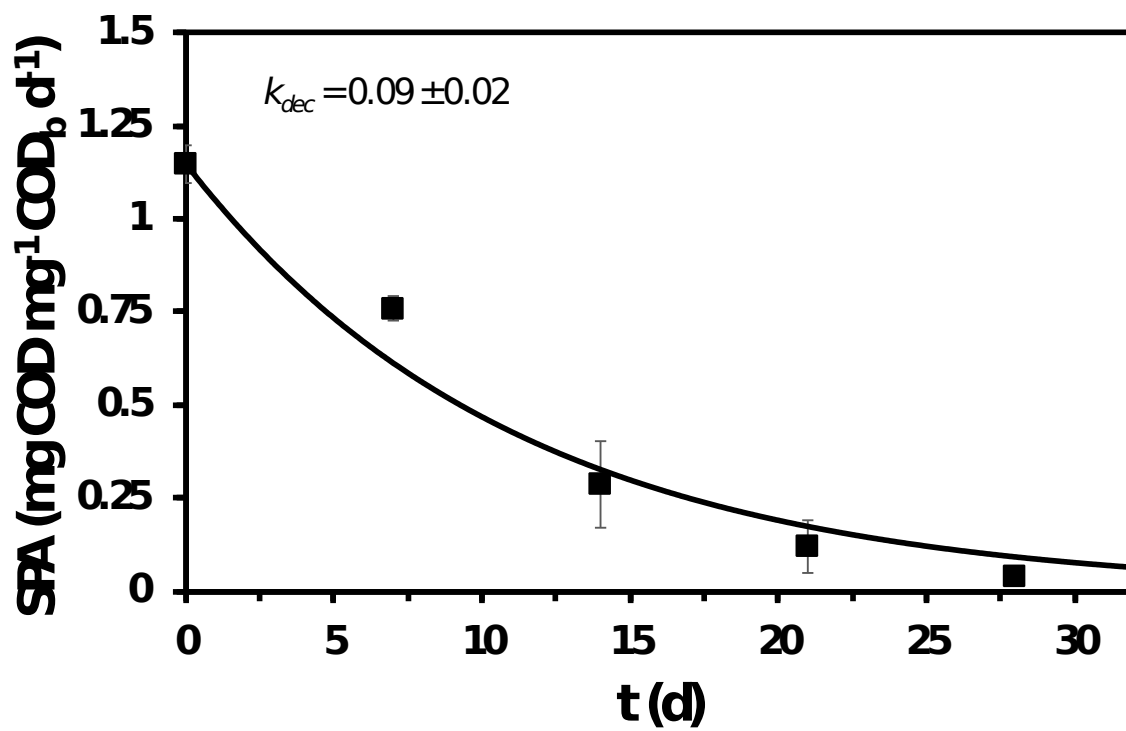
833 **FIGURE 2**



834

835

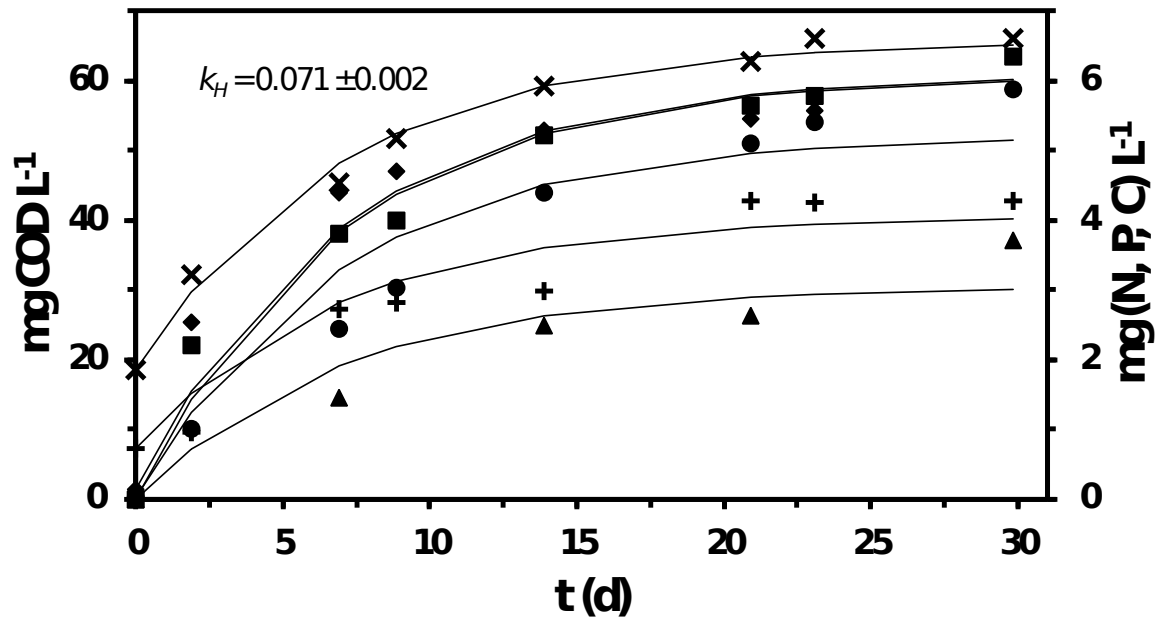
836 **FIGURE 3**



837

838

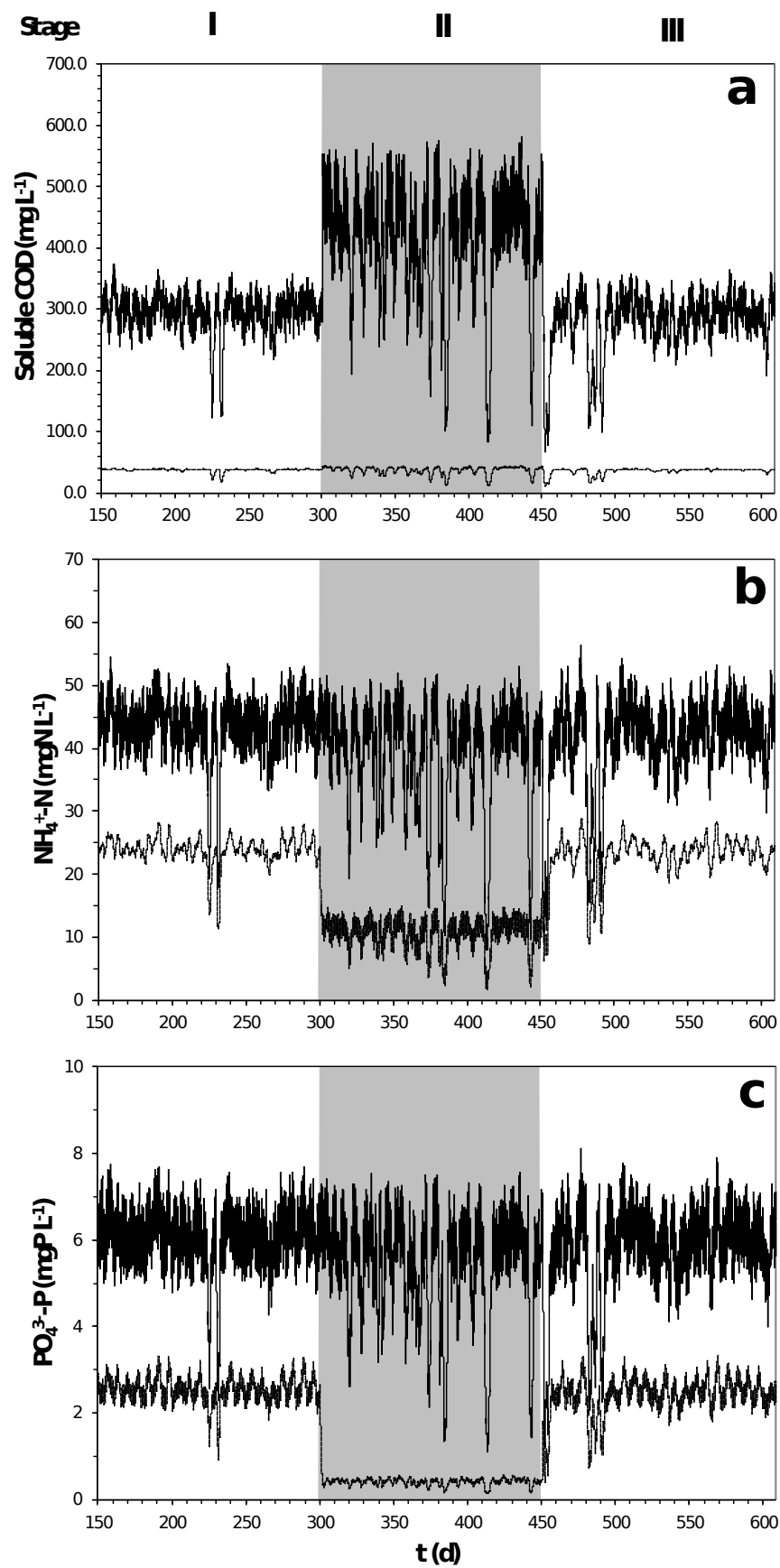
839 **FIGURE 4**



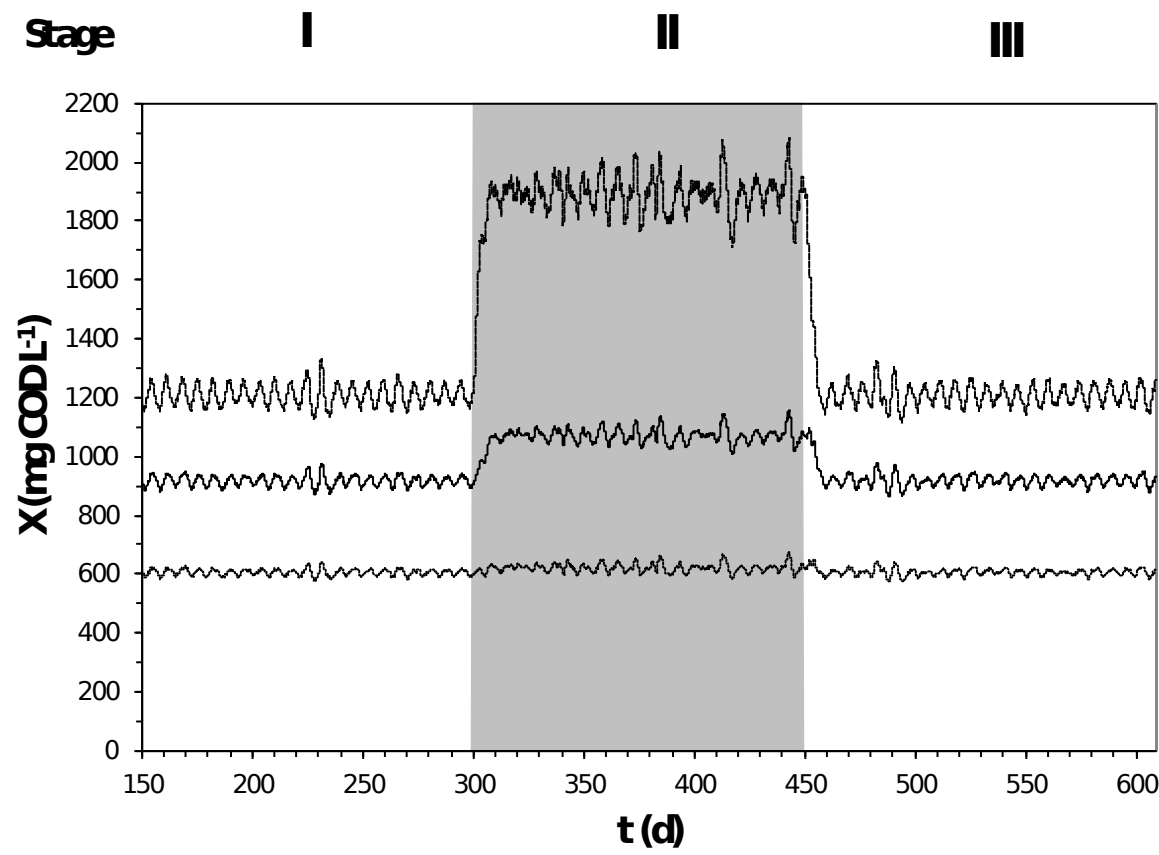
840

841

842 **FIGURE 5**



844 **FIGURE 6**



845

846

847

848